# Copper Conversion into $Cu(OH)_2$ Nanotubes for Positioning $Cu_3(BTC)_2$ MOF Crystals: Controlling the Growth on Flat Plates, 3D Architectures, and as Patterns

*Kenji Okada, Raffaele Ricco, Yasuaki Tokudome, Mark J. Styles, Anita J. Hill, Masahide Takahashi,* and Paolo Falcaro**

**A new approach for the fabrication of homogeneous HKUST-1 [$Cu_3(BTC)_2$] coatings on copper metal plates, 3D objects, and as patterns, is here proposed. The conversion can be performed at room temperature in approximately 30 minutes using an aqueous ethanolic mixture. The two step conversion mechanism occurs via the formation of $Cu(OH)_2$ nanotubes. Microscopic time-course monitoring reveals the conversion steps. The adhesion of the metal organic-framework (MOF) crystals, as well as the functional properties of the resulting supported catalyst, are successfully tested. The versatility of the conversion mechanism on different metal copper substrates is investigated as well; in particular, a photolithography protocol is proposed for the preparation of MOF patterns. This protocol offers several features (short processing time, applicability to any copper metal object, low cost of the equipment, room temperature conditions) that would make it favorable for basic research and industrial exploitation of MOF capabilities.**

## 1. Introduction

Metal organic-frameworks (MOFs) are an intriguing class of functional ultra porous materials; their tuneable architecture and chemical properties make them promising materials for gas storage and separation.[1] More recently they have shown great potential for sensing,[2] microelectronics,[3] biomedics,[4] optics,[5] and catalysis.[6] In order to exploit the unique properties of these ultra-porous crystals in advanced applications such as miniaturised multifunctional platforms, methods of accurately positioning MOFs in precise locations on a device need to be developed. Different protocols have been proposed in order to achieve spatial control, examples of which include self-assembled monolayer,[7] microfluidics,[8] contact printing,[9] and heterogeneous nucleation.[10] As a general concept in lithography, cheaper, faster and more versatile approaches are preferable.[11] Considering this requirement, and the current lithographic technology used for device fabrication, significant research effort is now being focused on combining MOF technology with approaches such as photolithography,[12] imprinting,[13] and spray coating.[14] An efficient strategy for the control of the MOF location is the positioning of the MOF precursors that can be subsequently converted by chemical strategies. A remarkable example was proposed by Ameloot et al.,[15] in which the authors took advantage of electrochemical metallic dissolution processes and showed how copper electrodes can be efficiently converted into HKUST-1 (also called $Cu_3(BTC)_2$, $H_3BTC$ = 1,3,5-benzenetricarboxylic acid). The requirement of an electrochemical process with a complex experimental setup of conduction salts and $N_2$ bubbling, limits the versatility of the method. A new trend in the field of positioning MOFs proposes the use of ceramic materials as precursors for the synthesis of Al-, Zn-, and Cu-based MOFs.[16–19] Accordingly, in the current paper we describe how to use $Cu(OH)_2$ nanotubes prepared from copper metal for a controlled rapid conversion into $Cu_3(BTC)_2$. The $Cu_3(BTC)_2$ crystals are shown to homogenously decorate the copper surface maintaining the shape of the original metallic object. Using this proposed protocol, this metal organic framework can be easily grown on flat, 3D architectured, or patterned substrates. Although its growth has already been reported on mesh-type substrates, the related synthetic procedures are both time expensive (e.g., few days) and energy consuming (e.g., heating processes are involved in the synthetic protocols).[20,21] The procedure reported here enables any metallic Cu object to be decorated with $Cu_3(BTC)_2$ MOF crystals and the synthesis can be performed at room temperature in less than 1 hour. Using this approach $Cu_3(BTC)_2$ MOF growth can be spatially controlled at the micrometer-scale, without the need for electric current, hazardous solvent (e.g., Dimethylformamide), or sophisticated equipment (e.g., autoclave). The only requirement is the control of the copper metal geometry and location. As current electronic technology utilises copper based conductive circuits, copper lithography is one of the most

K. Okada, Dr. Y. Tokudome, Prof. M. Takahashi
Department of Materials Science
Graduate School of Engineering
Osaka Prefecture University
Sakai, Osaka, 599–8531, Japan
E-mail: masa@photomater.com
Dr. R. Ricco, Dr. M. Styles, Dr. A. J. Hill, Dr. P. Falcaro
Division of Materials Science and Engineering
CSIRO, Private Bag 33, Clayton South MDC, Victoria, 3169, Australia
E-mail: Paolo.Falcaro@csiro.au

**DOI: 10.1002/adfm.201303303**

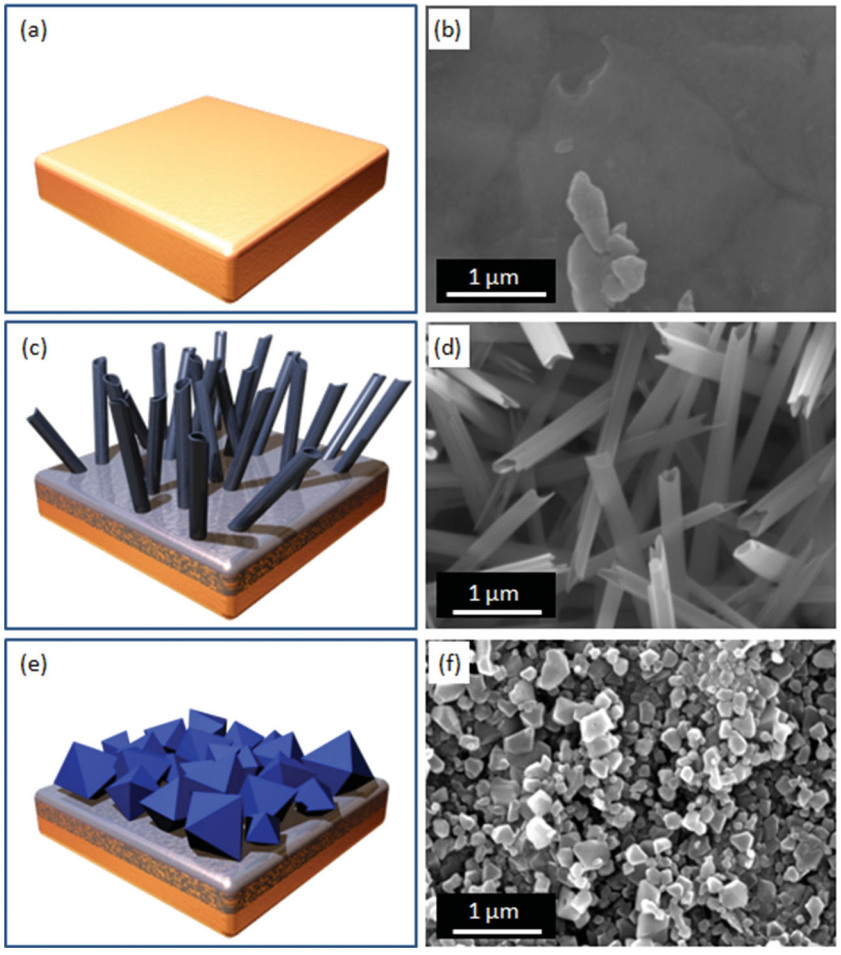


**Figure 1.** Schematic of the conversion process used to control the $Cu_3(BTC)_2$ growth on copper substrates. a) A copper substrate can be used, such as a copper plate. b) SEM image of the original Cu plate. c) After the treatment with NaOH and $(NH_4)_2S_2O_8$ in water, $Cu(OH)_2$ nanotubes are formed. d) The SEM image reveals the elongated hollow shape of $Cu(OH)_2$ nanotubes. e) MOF formation can be obtained by exposing the $Cu(OH)_2$ to the BTC ligand; f) SEM image of $Cu_3(BTC)_2$ crystals formed within 5 min.

cheap and fast photolithographic processes available. Many different types of protocols for the fabrication of copper-based miniaturized devices are readily available.[22,23] In this paper we show how 90 s of sunlight exposure, 30 min developing, and 35 min chemical conversion are enough to obtain printed circuit board (PCB)[23] MOF patterns. Without limitation of surface dimension/architecture or electrical connectivity of the copper support, a quick conversion into $Cu_3(BTC)_2$ can be now easily performed.

## 2. Results and Discussion

The procedure for the fabrication of $Cu_3(BTC)_2$ coatings is illustrated in **Figure 1**. The protocol can be described as a two step approach: the conversion from metallic copper to $Cu(OH)_2$ nanotubes, followed by the conversion of the copper hydroxide into Cu-based MOF $Cu_3(BTC)_2$. The copper hydroxide nanotubes were synthesized by following the procedure proposed by Zhang et al.[24] who describe how to fabricate single crystal nanotube arrays of $Cu(OH)_2$. After cleaning procedures of the precursor metal plate, the metallic copper was immersed into an aqueous solution of NaOH (sodium hydroxide) and $(NH_4)_2S_2O_8$ (ammonium persulfate). After 30 min of reaction the formation of $Cu(OH)_2$ nanotubes was detected. The transformation of the metallic substrate into nanotubes was observed using scanning electron microscopy (SEM) as shown in Figure 1b,d.

The second step requires the immersion of the $Cu(OH)_2$ nanotubes into an mixture of water, alcohol and 1,3,5-benzenetricarboxylic acid (trimesic acid, $H_3BTC$). During this final reaction the conversion from the ceramic material into a Cu-based MOF ($Cu_3(BTC)_2$) was performed within a few minutes at room temperature (Figure 1f). The mechanism has been recently reported by Majano et al.[17], who converted a commercial slurry of $Cu(OH)_2$ in water into HKUST-1 powders using an acid-base reaction ($3\ Cu(OH)_2 + 2\ H_3BTC \rightarrow Cu_3(BTC)_2 + 6\ H_2O$). However, the efficient conversion $Cu(OH)_2$ into MOFs by this approach required the homogenization of $Cu(OH)_2$ micronized powders, leading to the formation of powdery MOFs. In our study, we propose the direct growth of MOFs on a metallic substrate via copper hydroxide nanostructures that can be efficiently converted into MOF due to the specifically designed high surface area.

The conversion process from copper hydroxide to $Cu_3(BTC)_2$ has been investigated using SEM. The evolution of the copper hydroxide nanotubes in the presence of the ligand ($H_3BTC$) is reported in **Figure 2**. The use of nanotubes fixed on a substrate as precursors helped to reveal the conversion mechanism; the initial mechanism is similar to the one discovered by Reboul et al.[16] where the authors investigated the transformation from nanometer scale ceramic precursor into MOFs by electron microscopy time-course monitoring. Here we used a similar approach to collect snapshots of the changes occurring during the reaction between the $Cu(OH)_2$ and the $H_3BTC$ ligand. We identified three different main contributions to the MOF growth: pseudomorphic transformation, crystal growth and Ostwald ripening. Figure 2a shows $Cu(OH)_2$ nanotubes used as precursors for the MOF formation; the nanotubes are a few micrometers in length and present a smooth surface. After one second reaction time with the BTC ligand, the surface of the nanotubes becomes rough and wider in diameter due to the almost instantaneous growth of MOFs with average dimension < 200 nm (Figure 2b). Within 1 minute reaction time (Figures 2a–e), $Cu(OH)_2$ nanotubes rapidly converts to MOFs with bigger crystal size; the nanotubes become shorter vertical clusters of MOFs and the diameter increases as well as the roughness. At 25 s (Figure 2d)

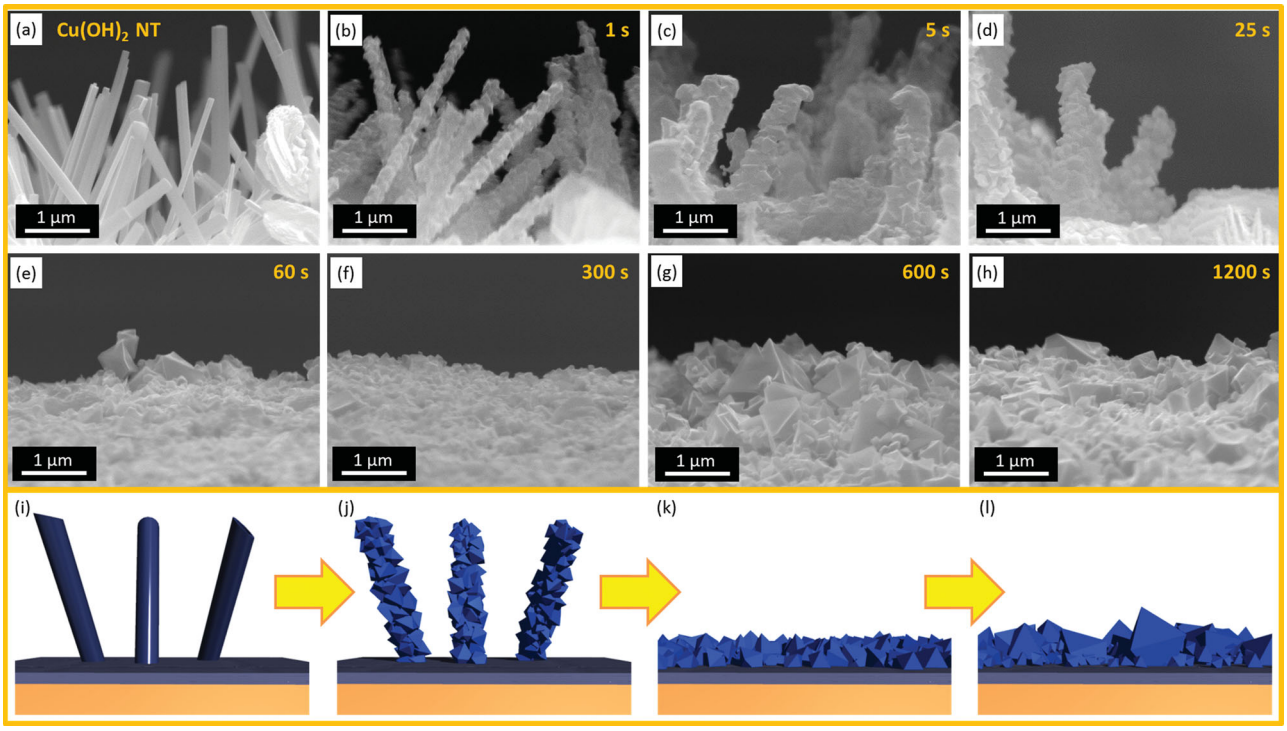


**Figure 2.** Evolution of the $Cu(OH)_2$ nanotubes from the original shape was investigated using SEM. a) The substrate decorated with $Cu(OH)_2$ nanotubes, once immersed in a 1,3,5-benzenetricarboxylic acid and alcoholic mixture, shows a rapid conversion into a crystalline material. b) The change can be detected within 1s. c–h) Further evolution leading towards the formation of a flat layer of MOF crystals. i–l) Schematic representing the key steps in the morphological change during the $Cu_3(BTC)_2$ crystal formation using $Cu(OH)_2$ nanotubes. i,j) Change dominated by the pseudomorphic replication. j–k) Crystal growth without the conservation of the initial tubular shape. k,l) Change dominated by the Ostwald ripening mechanism.

the typical crystal shape of $Cu_3(BTC)_2$ can be detected (see the Supporting Information, Figure S1). At 300 s (Figure 2f) no vertical crystal clusters are detected and the surface is flat and densely covered by MOFs. At this reaction time the crystal size ranges from 200 to 400 nm (Figure S1, Supporting Information). For longer reaction times, MOF crystals up to 1 µm can be measured (see the Supporting Information, Figure S2). The increased crystal size and film roughness with reaction time are shown; however, a reaction time longer than 600 s does not show significant changes (Figure 2g,h). At 600 s, crystals around 1 µm can be easily found along with smaller crystals. After 1200 s no significant change in the morphology is detected. Based on this observation, we think that the initial conversion from $Cu(OH)_2$ to MOFs occurs at the nanotube interface; a "dissolution–reprecipitation" mechanism dominates the conversion process in the initial stage maintaining the shape features of the initial nanotubes. This process would allow for the transition in the schematic from Figure 2i,j. It is important to note that the "dissolution-reprecipitation" mechanism described by Reboul et al.[16] maintains the architecture of the inorganic material used as the precursor of the corresponding MOF; for instance, $Al_2O_3$ inverse opal leads toward the formation of the corresponding MIL-53(Al) framework. From the configuration proposed in Figure 2j, the further crystal growth induces the formation of a homogeneous coating of MOFs where the crystals have similar dimensions (Figure 2k). The further reaction time with the ligand shows a change in the crystal size distribution (Figure 2l) suggesting a process dominated by Ostwald ripening.

X-ray diffraction (XRD) was performed to verify the crystalline structure. **Figure 3**a shows XRD pattern of $Cu_3(BTC)_2$ obtained from a copper plate after 300 s reaction time. The powder sample was collected by scraping the coating off the copper plate and the measurement was performed using a spinning capillary in Debye-Scherrer geometry. Based on a classical recipe reported in the literature, HKUST-1 was prepared following a solvothermal method from copper nitrate and $H_3BTC$ in a mixture of *N*,*N*-dimethylformamide (DMF), ethanol and water.[25] As shown in Figure 3a, the peaks of the obtained product correspond with those of $Cu_3(BTC)_2$ crystals prepared with the classical method; further confirmation is provided by a simulation that shows a full correspondence (see Supporting Information, Table S1). However, peaks related to residual $Cu(OH)_2$ and CuO are detected in the diffraction pattern. A weak copper metal signal was detected as well: this probably arises from the scratching procedure because a steel scalpel was used to detach the crystals from the metallic plate. Although a quantitative determination of the different copper based materials is not possible due to mismatches in the relative peak intensities and uncertainty regarding possible amorphous content, we roughly estimate that $Cu_3(BTC)_2$, $Cu(OH)_2$, CuO, and $Cu_{(m)}$ are present at 13, 25, 61, and 1 wt% respectively. The presence of CuO can be explained by the dehydration of the copper hydroxide and the presence of a base could accelerate the oxide formation.[24,26] The correspondence between the diffraction peaks of the MOF obtained using the solvothermal method and the conversion from $Cu(OH)_2$ was

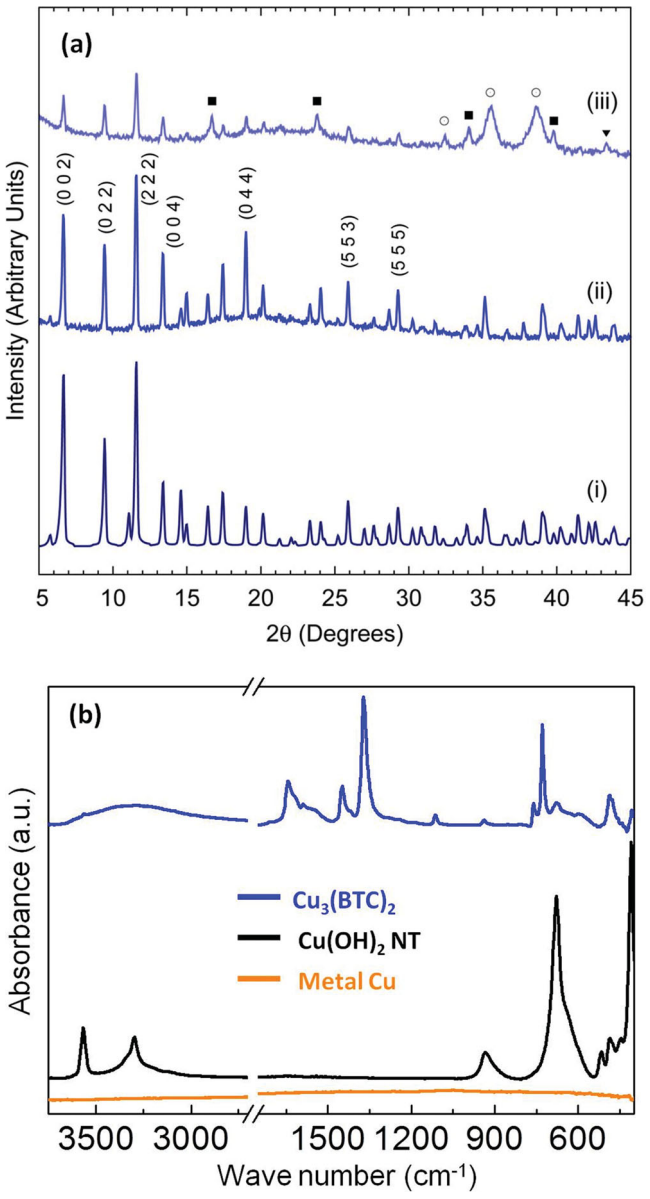


**Figure 3.** Characterization of the $Cu_3(BTC)_2$ coating prepared on a copper plate. a) XRD diffraction patterns of simulated $Cu_3(BTC)_2$ (i), $Cu_3(BTC)_2$ prepared with the standard solvothermal approach (ii); and the $Cu_3(BTC)_2$ prepared via $Cu(OH)_2$ nanotubes (iii). In this diffraction pattern, peaks are also assigned to CuO(■), $Cu(OH)_2$(○), FCC Cu (▼). b) FTIR spectra of initial metallic Cu (orange line), copper hydroxide nanotubes (black line) and $Cu_3(BTC)_2$ (blue line).

confirmed using small angle X-ray scattering as well (the diffraction patterns are reported in the Supporting Information, Figure S3).

FTIR (Fourier transform infrared spectroscopy) measurements in attenuated total reflectance (ATR) mode was performed on the metal plate, on the precursor $Cu(OH)_2$ nanotubes and on the $Cu_3(BTC)_2$ coating (Figure 3b). In the spectrum related to the copper hydroxide, the modes at 3570 and 3300 $cm^{-1}$ are attributed to the O–H stretching mode,[27] 934 and 678 $cm^{-1}$ are assigned to the O–H bending mode.[28] The remaining modes at 517, 487, 446, and 410 $cm^{-1}$ are assigned to the Cu–OH stretching mode.[29] After immersing the copper hydroxide in the conversion solution for 300 s, new peaks are detected and assigned to the organic molecules used as ligands in the $Cu_3(BTC)_2$ framework; 729, 760, 937 $cm^{-1}$: C–$CO_2$ stretching, 1114 $cm^{-1}$: C–O stretching, 1373, 1449, 1645 $cm^{-1}$ : COO–$Cu_2$ stretching.[30] This result indicates that the products are mainly composed of Cu-based MOF. However, a few peaks derived from $Cu(OH)_2$ (around 3570 and 680 $cm^{-1}$) remain, which is consistent with that obtained by XRD measurement.

From these characterizations, we can summarize that the $Cu_3(BTC)_2$ obtained here presents the typical crystalline structure and composition of the classical HKUST-1 prepared by solvothermal methods. However, residual $Cu(OH)_2$ can be detected from both, XRD and FTIR investigations while the CuO seems to be a byproduct of the method used for the $Cu(OH)_2$ nanotube formation.

A $N_2$ sorption analysis was performed on Cu meshes prior and after the $Cu(OH)_2$ and $Cu_3(BTC)_2$ conversion steps. The measured specific surface area was negligible for the pristine metallic copper mesh (≈0 $m^2 g^{-1}$), while 0.21 $m^2 g^{-1}$ were measured for the $Cu(OH)_2$ decorated mesh and 16.3 $m^2 g^{-1}$ for the $Cu_3(BTC)_2$ covered mesh (details are reported in the Supporting Information).

To test the adhesion properties of the framework on the substrate, three identical Cu plates with dimensions 20 mm × 10 mm were used for the generation of HKUST-1 via $Cu(OH)_2$ (300 s as reaction time). These coated plates were immersed in ethanol and sonicated for 5, 10, and 30 min respectively. The three samples were then investigated using SEM (**Figure 4**). No changes in the coating morphology were detected within 30 min; this result indicates that the MOFs prepared with the procedure reported here are efficiently anchored to the metal plate. The presence of residual $Cu(OH)_2$ detected by XRD and FTIR in the $Cu_3(BTC)_2$ coating might play an important role for the adhesion properties acting as an conversion layer between the substrate and the MOFs.

To explore the versatility of the technique with a different substrate, a copper mesh (200 µm wire diameters, 400 µm squared holes, **Figures 5**a–d) was used as a substrate for the MOF growth. Again the $Cu(OH)_2$ nanotubes were prepared using the previously described synthetic procedure. SEM images taken at various times during the processing are presented in the Supporting Information, Figure S4. After the final conversion into MOFs (300 s reaction time), the mesh presented an opaque blue color and rough surface to the naked eye. A closer look into the mesh wires reveals that the surface appears homogeneously covered by the crystals; the SEM images again show a layer composed of the typical $Cu_3(BTC)_2$ crystalline octahedral morphology.[31] Energy dispersive X-ray spectroscopy confirms the X-ray emission peaks from Copper (8.04 keV), Oxygen (0.525 keV), and Carbon (0.277 keV). In particular, performing a mapping analysis, Cu, O and C signals overlap along the entire investigated surface (Supporting Information, Figure S5). However, due to the shadow effect induced by the directional electron beam, it is shown that the presence of copper comes from both the metallic substrate and the MOFs grown onto it. Signals related to MOF elements overlap the typical crystal morphology detected by SEM. Substrates with

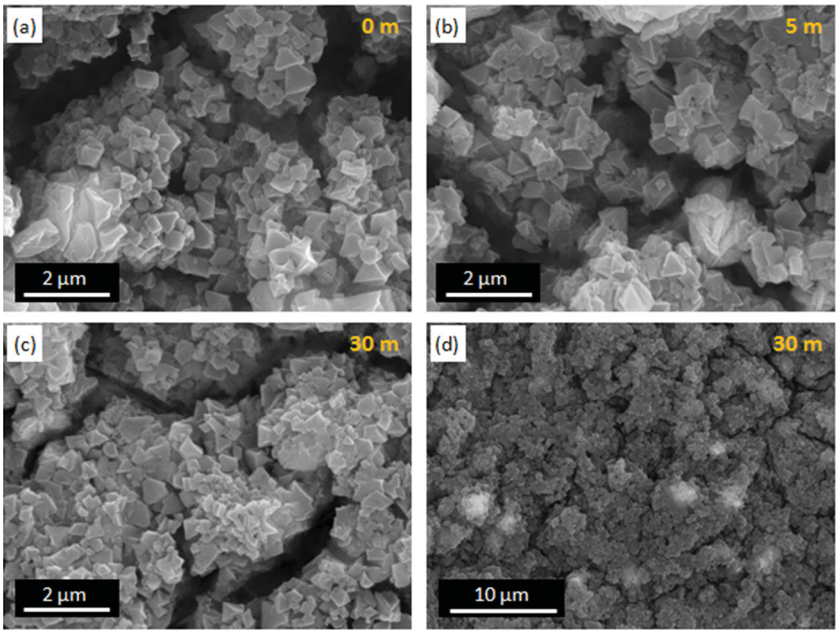


**Figure 4.** Investigation of the sonication effect on the MOF coating. No difference is detected by SEM even after 30 min highlighting how the $Cu_3(BTC)_2$ is not significantly affected by this mechanical sonication.SEM images of the: a) as made sample (0 min), b) sample sonicated for 5 minutes, and c) the sample sonicated for 30 minutes. d) Larger area of the sample after 30 minutes sonication.

different shapes were used to further perform the superficial conversion from Cu to $Cu(OH)_2$ and finally into $Cu_3(BTC)_2$. 3D miniaturized object was chosen to test the ability of the proposed protocol in the micrometer-scale. In Figure 5e,f, the successful conversion of a 30 µm wire and a 10 µm Cu grid (Figures 5g,h) is reported. This experiment shows how curvatures in the micrometer-scale (wire) and sharp edges (copper grid) do not affect the homogenous growth of the crystals. The illustrated resolution limit is 10 µm, corresponding to the copper grid thickness. This method could therefore be useful for the integration of supported $Cu_3(BTC)_2$ MOFs into multifunctional platforms. For example, miniaturized copper supports could be converted and then integrated; or alternatively integration of minitaturized copper could be accomplished if the device allows for in situ post-conversion (e.g., microfluidic circuits or micro-separators).

Although structural, compositional and elemental information confirms the $Cu_3(BTC)_2$ identity of the MOF crystals, it is important to test the functional properties of the assembly. A field that might take advantage of 3D architectured substrates homogeneously coated with a functional material is catalysis. Accessible catalytic materials supported by a mechanically stable substrate could help in positioning the active material into a reactor for chemical reaction yield improvement. $Cu_3(BTC)_2$ represents an ideal candidate for a variety of copper based catalytic reactions.[32] Here we present how such a MOF-supported catalyst can be used to accelerate the Friedländer reaction between 2-aminobenzophenones and acetylacetone following the schematic given in **Figure 6**. The Friedländer reaction[33] has been proposed as a catalytic test for $Cu_3(BTC)_2$ by Pérez-Mayoral et al.[34] and subsequently it has become an evaluation test for the catalytic properties of this Cu-based MOF.[35] It is important to note that this reaction is one important synthetic approach for the synthesis of quinolines, which are nitrogen

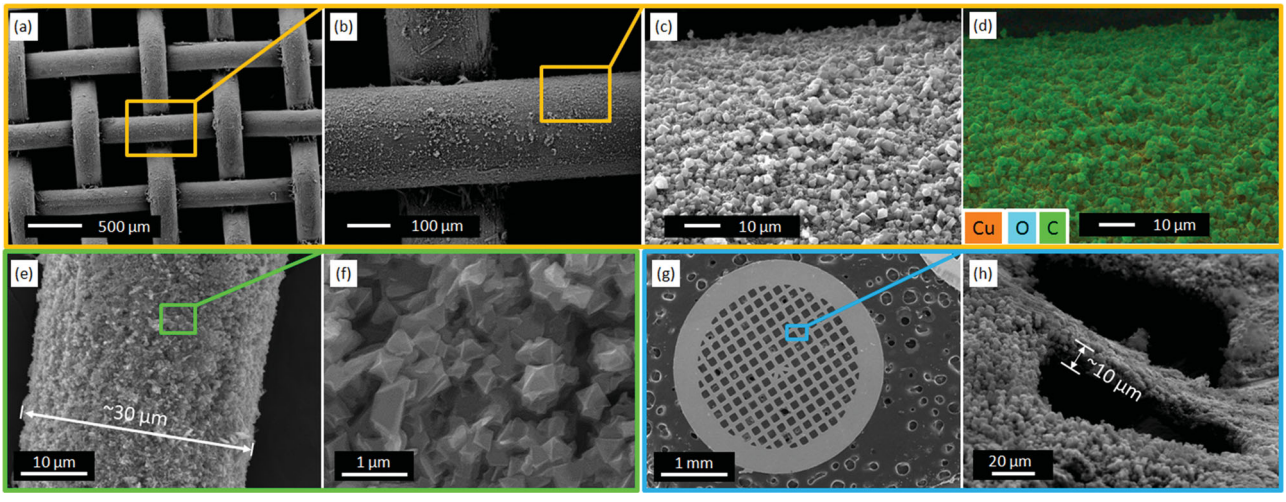


**Figure 5.** Morphological and elemental analysis performed on various copper substrates. a–d) A copper mesh morphology is presented at 3 different magnification (a–c); the energy dispersive X-ray analysis confirms the homogeneity of the $Cu_3(BTC)_2$ coating and the elemental composition (d) Cu: orange, O: light blue, C: green). e–h) SEM images of 3D copper objects with features in the micrometer-scale; e,f) 30 µm copper wire and g) a 2.5 mm $\phi \times 10$ µm copper grid have been homogeneously superficially decorated with $Cu_3(BTC)_2$. h) magnification of the tilted copper grid showing a part of grid in cross-section.

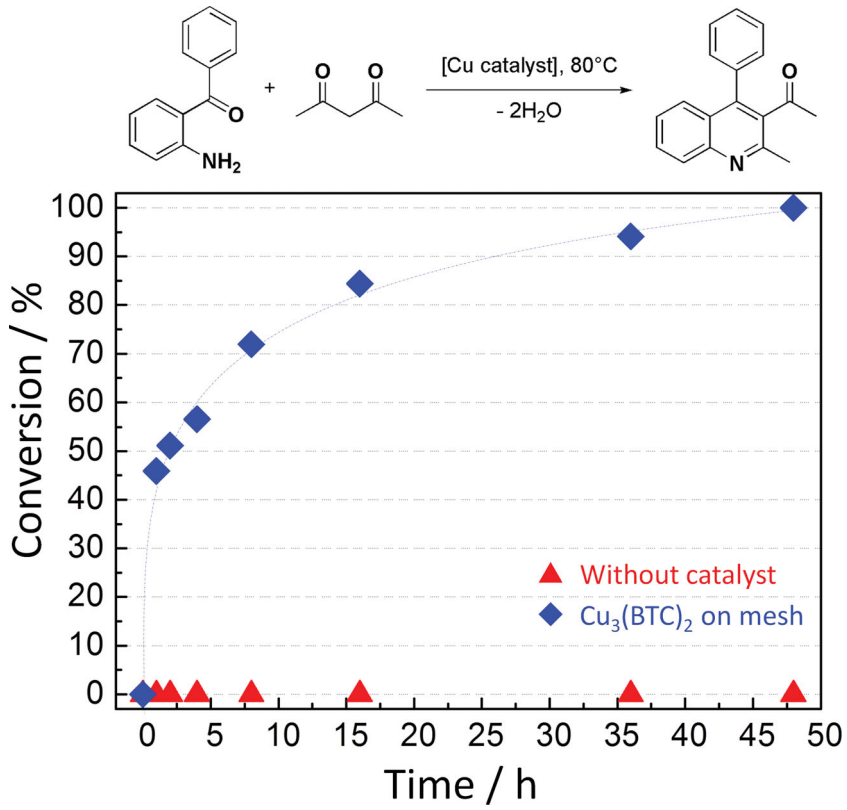


**Figure 6.** Friedländer reaction conversion (%) performed at 80 °C for reactants with $Cu_3(BTC)_2$ on copper mesh and without any catalyst. The system without any $Cu_3(BTC)_2$ catalyst shows no conversion at the detectable level, while the $Cu_3(BTC)_2$ decorated mesh enhances the conversion reaction.

heterocyclic compounds with significant pharmacological activities.[34,36] In addition, $Cu_3(BTC)_2$ has proven to be an efficient and environmental-friendly catalyst for such a reaction;[34] therefore, the ability to locate it on a solid support is one further step toward industrial applications exploiting the MOF properties. The reaction was performed at 80 °C using a solvent-free approach (the reactant acetylacetone was used to dissolve 2-aminobenzophenone) proposed for Basolite C300 (Sigma–Aldrich). In this commercial system, $Cu^{II}$ species were considered as the main active sites responsible for the catalytic conversion.[34] The mechanism involving $Cu_3(BTC)_2$ as a catalyst has been recently revealed by Čejika's group.[35] The experiment described here shows clear evidence for the catalytic reaction promoted by the copper mesh covered by $Cu_3(BTC)_2$ MOF crystals. In Figure 6, the reaction yield over time is presented. The mixture of reactants without any MOF or copper metal shows no conversion at a detectable level. Conversely, the $Cu_3(BTC)_2$ decorated mesh shows a significant catalytic activity. After 16 h reaction time, $Cu_3(BTC)_2$ supported on Cu mesh shows a yield exceeding 80%. The 100% conversion occurs within 48 h in presence of supported MOFs, while the reference mixture without any catalyst shows no significant conversion even after 48 h. Importantly, both the metallic copper mesh and $Cu(OH)_2$ supported on Cu mesh did not promote any significant catalytic reaction (data not shown); this supports that the reaction is accelerated by $Cu^{II}$ species in MOF crystalized on Cu mesh.

To further progress the field of positioning MOFs for device fabrication, photolithography was used for the fabrication of copper patterns. Such a photolithographic approach is widely used in electronics for the fabrication of printed circuit board (PCB).[23] While in electronics and microelectronics copper is normally used as a conductive material, for the current experiment it was used as the initial material for a controlled conversion into MOFs. This experiment aims to test the protocol on planar surfaces, allowing the selectivity of growth on copper and the definition of lateral resolution to be tested. A PCB exposed to our protocol is presented in **Figure 7**. The 125 µm strips correspond to copper converted initially into $Cu(OH)_2$ nanotubes and then into $Cu_3(BTC)_2$. A higher magnification shows that the strips are completely and homogenously covered by MOFs, while the dielectric area on the naked

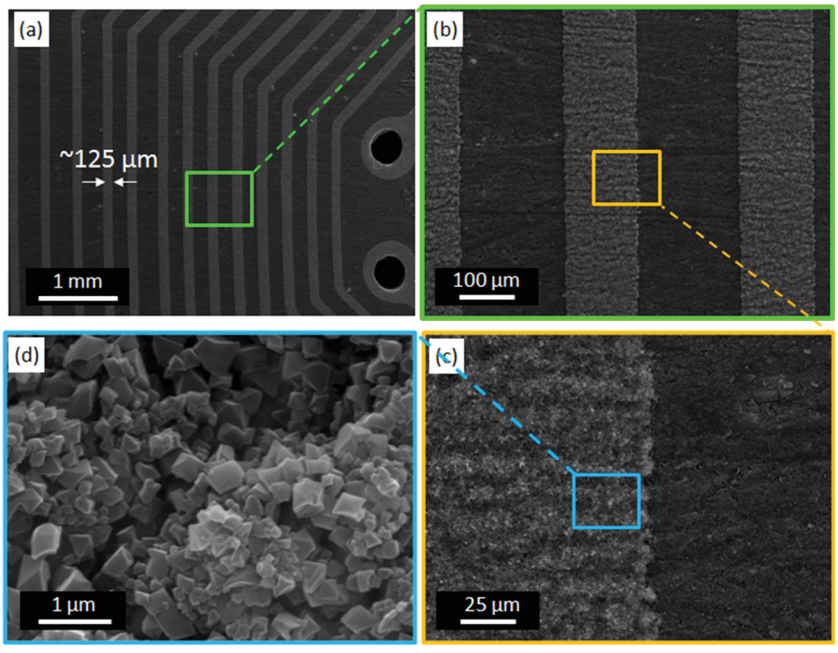


**Figure 7.** Conversion from a Cu pattern into $Cu_3(BTC)_2$ achieved on a printed electronic circuit board (PCB). The light gray parallel lines are made on copper decorated by MOF. The MOF growth occurs only on top of the copper.

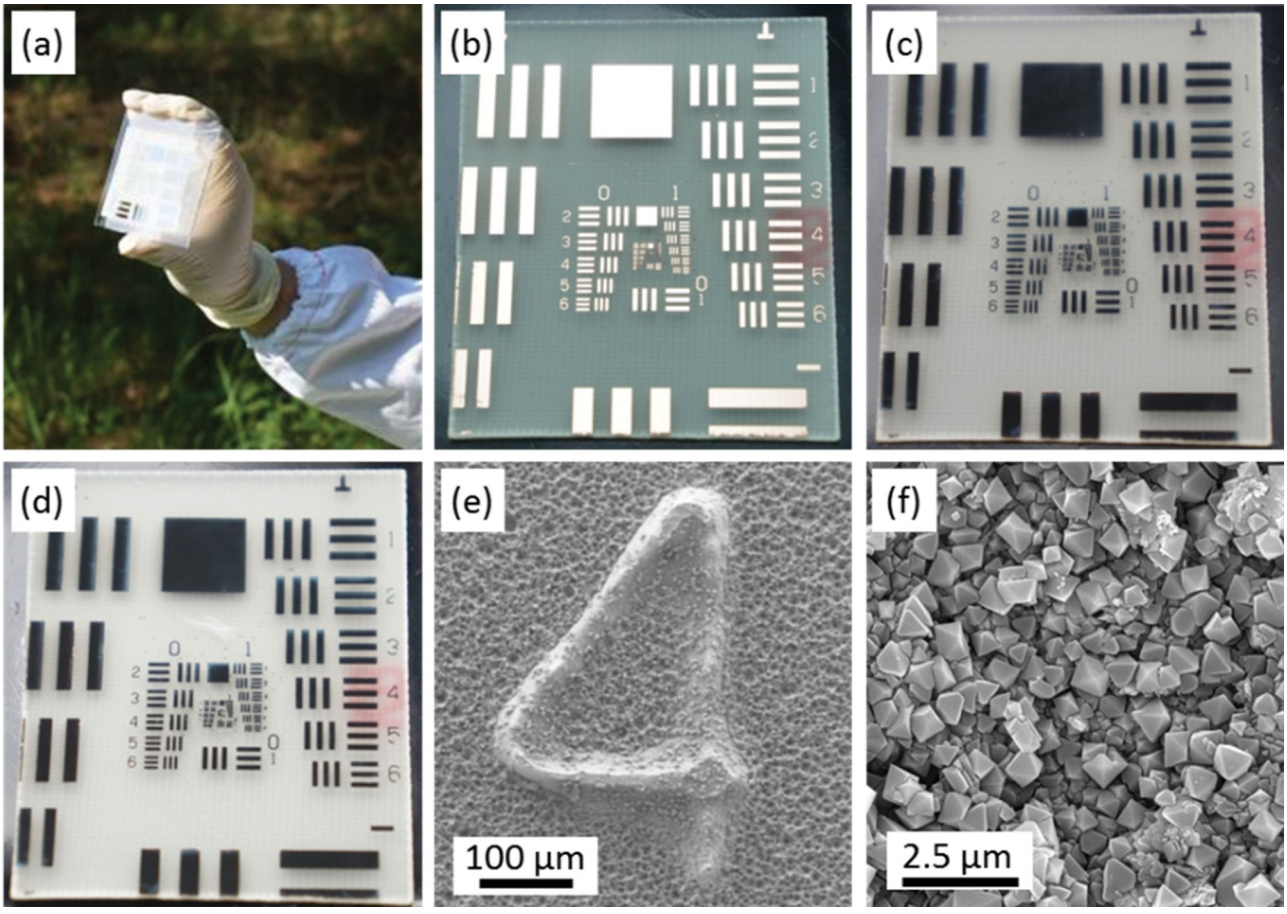


**Figure 8.** Preparation of $Cu_3(BTC)_2$ patterns using sunlight. a) A commercial resist coated copper board is covered with a UV-mask with a Cr pattern and exposed for 90 s to sunlight. b) The board is immersed into a developing solution (0.7 wt% NaOH aqueous solution) to remove the resist in the exposed regions, then a further immersion in $FeCl_3$ aqueous solution for around 15 min allows for the fabrication of a pattern. After washing with ethanol, the pattern is ready for the conversion into c) $Cu(OH)_2$ nanotubes and d) finally into $Cu_3(BTC)_2$. e) The SEM image shows the resolution obtained with this protocol and f) an image with higher magnification shows the $Cu_3(BTC)_2$ MOF crystals decorating the surface.

support (woven glass fiber epoxy composite, FR-4[37] does not show any MOF crystals. From our SEM measurements, the lateral resolution of this industrial substrate is considered to be approximately 5 µm.

Although the use of UV-lithography equipment for the patterning of resist coated copper PCB can be considered as a relatively cheap fabrication method, we further proved the extreme versatility of the proposed protocol using sunlight as a radiation source to pattern the photoresist layer on commercial PCB laminated copper boards. Under sunlight exposure with a commercial UV-mask, 90 s exposure time is enough to achieve patterns with features in the tens of micrometer scale (**Figure 8**). In less than 30 min, it is then possible to achieve the copper pattern firstly etching the photoresist in the sunlight exposed regions and secondly removing the copper metal from such areas by acid solution (Figure 8b). The further conversion into $Cu(OH)_2$ nanotubes and $Cu_3(BTC)_2$ is presented in Figure 8c,d. The SEM images confirm the presence of isolated copper patterns fully decorated by MOFs.

With this protocol it is now possible to produce $Cu_3(BTC)_2$ patterns using current technology; nevertheless it is also possible to fabricate patterns based on $Cu_3(BTC)_2$ with minimum equipment, such as an UV mask and a commercial resist coated copper PCB board. This protocol offers easy access to patterned MOFs for the exploration of MOF properties in miniaturized devices and the possibility to develop an industrial protocol using this environmentally friendly approach.

## 3. Conclusion

In this work, we presented a straightforward protocol for the preparation of $Cu_3(BTC)_2$ decorated copper metal. The process is environmentally friendly because the only organic solvent used is ethanol. The procedure requires approximately 30 min if the copper substrate is ready for the conversion; the MOF properties are maintained as shown by using copper mesh covered superficially with $Cu_3(BTC)_2$ to catalyze the Friedländer reaction. Due to the mild synthesis conditions (room temperature) this process can be potentially applied to a variety of substrates. In this paper we showed how the conversion can be successfully applied to a flat surface in the centimeter scale down to

3D objects with features in the micrometer scale. The MOF crystals formed by the conversion of $Cu(OH)_2$ nanotubes into $Cu_3(BTC)_2$ are mechanically resistant to sonication, suggesting a good adhesion with the substrate. Additionally, the procedure allows for the fabrication of MOFs on isolated patterns without electrical connectivity of the copper support because the conversion requires no electric current. Due to the current microelectronic technology based on copper, the fabrication of Cu-based MOF is very accessible; with a commercial photoresist coated copper board (around 12€ for 10 cm × 15 cm board), the entire patterning procedure requires approximately 1.5 h and it can be performed using sunlight. The versatility towards different substrates (including waste copper), the short processing time, the environmentally friendly synthetic conditions, and the low cost of equipment combine to make this protocol a promising procedure for the preparation of Cu-based MOF films and patterns for industrial applications.

## 4. Experimental Section

*Synthesis of $Cu_3(BTC)_2$ from Metallic Copper via $Cu(OH)_2$*: Copper substrates were purchased form RS-Components (e.g., naked and resist coated copper substrates, RS components CODE : 159–5773). Ethanol, NaOH, $(NH_4)_2S_2O_8$, 1,3,5-benzenetricarboxylic acid (trimesic acid, $H_3BTC$) were purchased from Acros Organics.

The solution for conversion from metal to hydroxide was prepared by mixing 4 mL of 10 m NaOH solution, 2 mL of 1 m $(NH_4)_2S_2O_8$ solution and 9 mL of deionized water without the need of additional solvent.[24] A clean metal copper plate (20 mm × 10 mm) was immersed into the mixed solution for 30 min at room temperature. After 30 min, the copper precursor was removed from the solution and then washed with water and ethanol. The as-prepared copper hydroxide nanotubes were dried and stored under ambient condition. The conversion from copper hydroxide to $Cu_3(BTC)_2$ was performed at room temperature by immersing the obtained copper hydroxide nanotube decorated copper metal into a ligand solution (1.8 mL of water, 4.67 mL of ethanol mixture, 0.21 g of $H_3BTC$).[17] Typically, after 5 min, the product was removed from the solution and washed with water and ethanol, then dried under air.

To investigate the evolution of the MOF growth, eight Cu 40 meshes (200 μm wire diameters, 400 μm squared holes) decorated with copper hydroxide nanotubes were immersed into the MOF conversion solution, and then at a certain time one sample was removed out from the solution and immediately washed with water and ethanol, then dried and stored in ambient conditions. The same procedure was used for the conversion of Cu 100 mashes (110 μm wire diameters).

The resistance test for adhesive properties was performed using $Cu_3(BTC)_2$ synthesized at 300 s reaction time on Cu plates (20 mm × 10 mm). The MOFs on three substrates in ethanol were sonicated for 5, 10, and 30 min, respectively. After that, each sample was washed with ethanol and dried under air.

To check the versatility of our reported synthesis protocol, the conversion from metallic copper into $Cu_3(BTC)_2$ via copper hydroxide nanotubes was performed using initial metallic copper with different 3D-architectures; wire-type metallic copper with ≈30 μm diameter prepared by etching copper wire with ≈110 μm initial diameter in $FeCl_3$ aqueous solution (15 g $FeCl_3$ in 25 mL water) for 7 min and a clean TEM grid. The conversion process from metallic Cu into copper hydroxide and from $Cu(OH)_2$ into Cu-based MOFs is confirmed as the same procedures as described above.

*Fabrication of Patterned $Cu_3(BTC)_2$ Film*: For a test of substrate selectivity and the definition of the lateral resolution of patterning MOFs, a DDR memory board (as-pattered PCB) was used as the initial Cu precursor after polishing the surface with sandpaper to expose the metallic copper to the reaction solution (polishing remove the surface resist layer which is composed of epoxy or epoxy-acrylate resin). To make patterned Cu substrates by photolithography using sun light as the radiation source, a commercial resist coated copper substrate (RS components CODE : 159–5773) was covered with a photomask with a Cr pattern and exposed to sunlight for 90 s. Then, the substrate was immersed into 0.7 wt% aqueous NaOH solution to remove the photoresist in the exposed regions, then a further immersion in aqueous $FeCl_3$ solution (15 g $FeCl_3$ in 25 mL water) for around 15 min allows for the fabrication of a pattern. After washing the remaining photoresist with ethanol, the patterned Cu board is ready for the conversion. The conversion procedure for patterned Cu into $Cu(OH)_2$ and from the copper hydroxide into $Cu_3(BTC)_2$ is the same as the one described above.

*Synthesis HKUST-1 Following the Conventional Solvothermal Approach (Reference Sample)*: HKUST-1 MOFs were prepared by conventional solvothermal methods by following the procedure proposed by Millward et al.[25] as a reference for the diffraction patterns for XRD investigation. Following this procedure, $Cu(NO_3)_2{\cdot}2.5H_2O$ (0.1 g) and $H_3BTC$ (0.05 g) were dissolved in 2.5 mL of mixed solution of DMF, ethanol and water (1 : 1 : 1). The solution was heated at 85 °C for 20 h. The obtained blue crystals were washed with fresh DMF and stored in DMF. It is important to highlight that DMF was used just for this solvothermal synthesis.

*Test of Catalytic Activities*: Friedländer reaction was catalyzed by $Cu_3(BTC)_2$ decorated copper 100 mesh (originally 6.32 g of pure copper). The samples, placed in a bottle, were activated at 100 °C under vacuum overnight before catalytic test. A reaction solution was prepared by mixing of 2-aminobenzophenone (7.88 g, 40 mmol) in acetylacetone (20.5 mL, 200 mmol). After immersion of the $Cu_3(BTC)_2$ on copper mesh in the 5 mL reactant mixture, the vessel was placed at 80 °C. As a reference sample, 5 mL of reactant solution without $Cu_3(BTC)_2$ catalyst in a vessel was placed in the heating bath. A volume corresponding to 0.2 mL of solution was collected from each bottle after 1, 2, 4, 8, 16, 36, 48 h. Prescribed volumes of solution were dried under vacuum at 70 °C, then diluted with 1 mL of $CDCl_3$ and analyzed with a Varian Unity Inova 300 NMR spectrometer. The most suitable integrals used to evaluate the catalytic activity were found for the signals at ≈6.5 ppm (proton in position 3 for the benzophenone reactant) and ≈8.1 ppm (proton in position 8 for the quinoline product).

*Characterization*: Surface morphologies of samples were observed using a scanning electron microscope (SEM, with a thin Iridium coating); the energy dispersive X-ray analysis has been performed using 20 KeV. Diffraction patterns of $Cu_3(BTC)_2$ were identified by X-ray diffraction (XRD; Philips) using CuKα radiation ($\lambda$ = 0.154 nm). Fourier transform infrared spectroscopy (FT-IR: ALPHA FT-IR spectrometer, Bruker Optik GmbH) was employed in the ATR configuration.

*Measurements of the Surface Area*: Copper mesh (100 mesh, 110 μm diameter wires) was received from Nilaco Co. Ltd and used without further treatment. The mesh was cut and rolled in three rolls. While one roll was left without any further treatment (Cu roll), the other two rolls were superficially converted into $Cu(OH)_2$ nanotubes. Finally, one of the two $Cu/Cu(OH)_2$ rolls was converted into MOF originating a $Cu/Cu(OH)_2/Cu_3(BTC)_2$ roll. The procedure used for the conversion is previously described. The three rolls were left at 150 °C under vacuum for 16 hours, following the activation procedure proposed by Majano et al.[17] The three rolls (approximately 1.7 g) were investigated by $N_2$ adsorption–desorption apparatus (BELSORP-mini II, Bel Japan Inc., Japan).

After measuring the BET specific surface area, portions of $Cu/Cu(OH)_2$ and $Cu/Cu(OH)_2/Cu_3(BTC)_2$ rolls were cut and investigated using thermogravimetric analysis. Thermogravimetric-differential thermal analysis (TG-DTA; Thermo Plus Evo, Rigaku, Japan) was carried out at a ramp rate of 5 K $min^{-1}$ under $N_2$ atmosphere at a flow rate of 300 mL $min^{-1}$. An estimation of the $Cu_3(BTC)_2$ weight was calculated as proposed in the supporting information. Based on such a weight and the surface area obtained by BET, the specific surface area of $Cu_3(BTC)_2$ on $Cu/Cu(OH)_2/Cu_3(BTC)_2$ was calculated.

## Supporting Information

Supporting Information is available from the Wiley Online Library or from the author.

## Acknowledgements

M.T. and P.F. acknowledge Australia-Japan ERLEP administrated by ATSE-EAJ-JSPS. P.F. acknowledges the Australian Research Council (ARC, DECRA Grant DE120102451), the AMTCP scheme, and the OCE science team for the Julius Award. The present work is partially supported by Grand-in-Aids from the Ministry of Education, Culture, Sports, Science and Technology (MEXT), administrated by Japan Society for the Promotion of Science (JSPS) (No. 22360276, No. 2510817). Part of this research was undertaken on the SAXS beamline at the Australian Synchrotron, Victoria, Australia with the support of Dr. Nigel Kirby and Dr. Adrian Hawley. The authors acknowledge Yuhi Yoshii, Naoki Tarutani, S. H. Skebest for helpful discussions.

Received: September 25, 2013
Revised: October 20, 2013
Published online: December 4, 2013

[1] K. Sumida, D. L. Rogow, J. A. Mason, T. M. McDonald, E. D. Bloch, Z. R. Herm, T.-H. Bae, J. R. Long, *Chem. Rev.* **2011**, *112*, 724.
[2] L. E. Kreno, K. Leong, O. K. Farha, M. Allendorf, R. P. Van Duyne, J. T. Hupp, *Chem. Rev.* **2012**, *112*, 1105.
[3] P. Falcaro, D. Buso, A. J. Hill, C. M. Doherty, *Adv. Mater.* **2012**, *24*, 3153.
[4] P. Horcajada, R. Gref, T. Baati, P. K. Allan, G. Maurin, P. Couvreur, G. Férey, R. E. Morris, C. Serre, *Chem. Rev.* **2011**, *112*, 1232.
[5] Y. Cui, Y. Yue, G. Qian, B. Chen, *Chem. Rev.* **2012**, *112*, 1126.
[6] J. Y. Lee, O. K. Farha, J. Roberts, K. A. Scheidt, S. B. T. Nguyen, J. T. Hupp, *Chem. Soc. Rev.* **2009**, *38*, 1450.
[7] a) S. Hermes, F. Schröder, R. Chelmowski, C. Wöll, R. A. Fischer, *J. Am. Chem. Soc.* **2005**, *127*, 13744; b) J. L. Zhuang, K. Lommel, D. Ceglarek, I. Andrusenko, U. Kolb, S. Maracke, U. Sazama, M. Fröba, A. Terfort, *Chem. Mater.* **2011**, *23*, 5366.
[8] D. Witters, N. Vergauwe, R. Ameloot, S. Vermeir, D. De Vos, R. Puers, B. Sels, J. Lammertyn, *Adv. Mater.* **2012**, *24*, 1316.
[9] a) C. Carbonell, I. Imaz, D. Maspoch, *J. Am. Chem. Soc.* **2011**, *133*, 2144; b) R. Ameloot, E. Gobechiya, H. Uji-I, J. A. Martens, J. Hofkens, L. Alaerts, B. F. Sels, D. E. De Vos, *Adv. Mater.* **2010**, *22*, 2685.
[10] a) P. Falcaro, A. J. Hill, K. M. Nairn, J. Jasieniak, J. I. Mardel, T. J. Bastow, S. C. Mayo, M. Gimona, D. Gomez, H. J. Whitfield, R. Riccò, A. Patelli, B. Marmiroli, H. Amenitsch, T. Colson, L. Villanova, D. Buso, *Nat. Commun.* **2011**, *2*, 237; b) C. M. Doherty, D. Buso, A. J. Hill, S. Furukawa, S. Kitagawa, P. Falcaro, *Acc. Chem. Res.*, DOI: 10.1021/ar400130a.
[11] P. Falcaro, D. Buso, A. J. Hill, C. M. Doherty, *Adv. Mater.* **2012**, *24*, 3153.
[12] a) C. Dimitrakakis, B. Marmiroli, H. Amenitsch, L. Malfatti, P. Innocenzi, G. Grenci, L. Vaccari, A. J. Hill, B. P. Ladewig, M. R. Hill, P. Falcaro, *Chem. Commun.* **2012**, *48*, 7483; b) G. Lu, O. K. Farfa, W. Zhang, F. Huo, J. T. Hupp, *Adv. Mater.* **2012**, *24*, 3970.
[13] C. M. Doherty, G. Grenci, R. Riccò, J. I. Mardel, J. Reboul, S. Furukawa, S. Kitagawa, A. J. Hill, P. Falcaro, *Adv. Mater.* **2013**, *25*, 4701.
[14] J.-L. Zhuang, D. Ar, X.-J. Yu, J.-X. Liu, A. Terfort, *Adv. Mater.* **2013**, *25*, 4631.
[15] R. Ameloot, L. Stappers, J. Fransaer, L. Alaerts, B. F. Sels, D. E. De Vos, *Chem. Mater.* **2009**, *21*, 2580.
[16] J. Reboul, S. Furukawa, N. Horike, M. Tsotsalas, K. Hirai, H. Uehara, M. Kondo, N. Louvain, O. Sakata, S. Kitagawa, *Nat. Mater.* **2012**, *11*, 717.
[17] G. Majano, J. Pérez-Ramírez, *Adv. Mater.* **2013**, *25*, 1052.
[18] W. W. Zhan, Q. Kuang, J. Z. Zhou, X. J. Kong, Z. X. Xie, L. S. Zheng, *J. Am. Chem. Soc.* **2013**, *135*, 1926.
[19] I. Stassen, N. Campagnol, J. Fransaer, P. M. Vereecken, D. E. De Vos, R. Ameloot, *Cryst. Eng. Commun.* **2013**, *15*, 9308.
[20] H. Guo, G. Zhu, I. J. Hewitt, S. Qiu, *J. Am. Chem. Soc.* **2009**, *131*, 1646.
[21] T. R. C. Van Assche, G. Desmet, R. Ameloot, D. E. De Vos, H. Terryn, J. F. M. Denayer, *Microporous Mesoporous Mater.* **2012**, *158*, 209.
[22] P. Maheshwari, *Electronic Components and Processes*, New Age International Publisher, New Delhi, India **2006**.
[23] R. S. Khandpur, Printed circuit boards: design, fabrication, assembly and testing, Tata-McGraw Hill, New Delhi, India **2005**.
[24] W. Zhang, X. Wen, S. Yang, Y. Berta, Z. L. Wang, *Adv. Mater.* **2003**, *15*, 822.
[25] A. R. Millward, O. M. Yaghi, *J. Am. Chem. Soc.* **2005**, *127*, 17998.
[26] Y. Cudennec, A. Lecerf, *Solid State Sci.* **2003**, *5*, 1471.
[27] I. Y. Park, K. Kuroda, C. Kato, *Solid State Ionics* **1990**, *42*, 197.
[28] a) A. Yin, X. Guo, W. L. Dai, K. Fan, *J. Phys. Chem. C* **2009**, *113*, 11003; b) T. Toupance, M. Kermarec, J. F. Lambert, C. Louis, *J. Phys. Chem. B* **2002**, *106*, 2277.
[29] a) R. L. Frost, *Spectrochim. Acta, Part A* **2003**, *59*, 1195; b) R. L. Frost, W. Martens, J. T. Kloprogge, P. A. Williams, *J. Raman Spectrosc.* **2002**, *33*, 801; c) K. Mudalige, M. Trenary, *J. Phys. Chem. B* **2001**, *105*, 3823.
[30] a) J. L. C. Rowsell, O. M. Yaghi, *J. Am. Chem. Soc.* **2006**, *128*, 1304; b) S. Loera-Serna, L. López-Núñez, J. Flores, R. López- Simeon, H. I. Beltrán, *RSC Adv.* **2013**, *3*, 10962; c) S. Loera-Serna, M. A. Oliver-Tolentino, M. de Lourdes López-Núñez, A. Santana-Cruz, A. Guzmán-Vargas, R. Cabrera-Sierra, H. I. Beltrán, J. Flores, *J. Alloys Comp.* **2012**, *540*, 113.
[31] E. Biemmi, S. Christian, N. Stock, T. Bein, *Microporous Mesoporous Mater.* **2009**, *117*, 111.
[32] L. Alaerts, E. Séguin, H. Poelman, F. Thibault-Starzyk, P. A. Jacobs, D. E. De Vos, *Chem. Eur. J.* **2006**, *12*, 7353.
[33] R. M. Martín-Aranda, J. Čejika, *Top Catal.* **2010**, *53*, 141.
[34] E. Pérez-Mayoral, J. Čejika, *ChemCatChem* **2011**, *3*, 157.
[35] a) E. Pérez-Mayoral, Z. Musilova, B. Gil, B. Marszalek, M. Polozij, P. Nachtgall, J. Čejika, *Dalton Trans.* **2012**, *41*, 4036; b) A. Sachse, R. Ameloot, B. Coq, F. Fajula, B. Coasne, D. De Vos, A. Galarneau, *Chem. Commun.* **2012**, *48*, 4749.
[36] J. Marco-Contelles, E. Perez-Mayoral, A. Samadi, M. do Carmo Carreiras, E. Soriano, *Chem. Rev.* **2009**, *109*, 2652.
[37] INDUSTRIAL LAMINATING THERMOSETTING PRODUCTS Database (NEMA LI 1, 98 00/00/11).